

High-Yield Synthesis of Monodisperse Dumbbell-Shaped Polymer Nanoparticles

Jin-Gyu Park,[†] Jason D. Forster,[†] and Eric R. Dufresne^{*,†,‡,§,||}

Departments of Mechanical Engineering, Chemical Engineering, Physics, and Cell Biology, Yale University, New Haven, Connecticut 06511

Received March 2, 2010; E-mail: eric.dufresne@yale.edu

Suspensions of highly uniform anisotropic nanoparticles have tremendous potential for use in materials science and engineering.¹ Their optical anisotropy opens new directions in photonic materials.² Similarly, they facilitate the visualization and understanding of condensed phases.³ However, the synthesis of uniform nonspherical particles is difficult in general because surface tension, which becomes more important as length scales decrease, favors spherical shapes. This limitation may be overcome with several techniques, such as clusterization⁴ and random coagulation.⁵ These techniques, however, generally require a separate sorting process to obtain uniform samples.

Seeded suspension polymerization is another strategy for producing nonspherical particles.⁶ In this approach, cross-linked spherical seed particles are first swollen with monomer and then collapse to form an additional lobe during heating and polymerization. This process typically results in particles with dimensions on the order of a few micrometers. Recently, a modified procedure for making submicrometer nonspherical particles was reported.⁷ In that process, the seed particles have a core-shell structure, with a highly cross-linked polystyrene (PS) core and a hydrophilic polymeric shell. Upon swelling and polymerization, they form ellipsoids and dumbbell-shaped particles with aspect ratios [i.e., length/diameter (L/D) ratios] as high as 1.3. In seeded suspension polymerization, it is generally assumed that cross-linking of the seed particles is a prerequisite for the formation of nonspherical shapes.

Here we present a method for producing highly monodisperse dumbbell-shaped polymer nanoparticles with dimensions on the order of a few hundred nanometers and tunable aspect ratios as high as 1.8. Similar to ref 7, we start with core-shell particles having a hydrophobic core and a hydrophilic shell. However, in our process, the seed-particle cores are not cross-linked. This synthesis features extremely high yields of stable nanoparticles.

We fabricated uniform dumbbell-shaped nanoparticles by two-step seeded emulsion polymerization, as summarized in Figure 1a. Starting with PS spheres (shown in Figure 1b), we synthesized spherical core-shell nanoparticles (shown in Figure 1c) through seeded emulsion polymerization. The shell is a random copolymer of styrene (St) and trimethoxysilylpropylacrylate (TMSPA).⁸ In the next step, we swelled the core-shell particles with styrene and polymerized them. The resulting particles displayed a highly uniform dumbbell shape on the scale of 250 to 500 nm, as shown in Figure 1d.

The core-shell nanoparticles showed intriguing behavior during swelling, which played a crucial role in our synthesis. This behavior is summarized in Figure 2, where we compare the swelling capability of PS nanoparticles, poly(St-co-TMSPA) nanoparticles, and core-shell nanoparticles by mixing them with toluene for 20

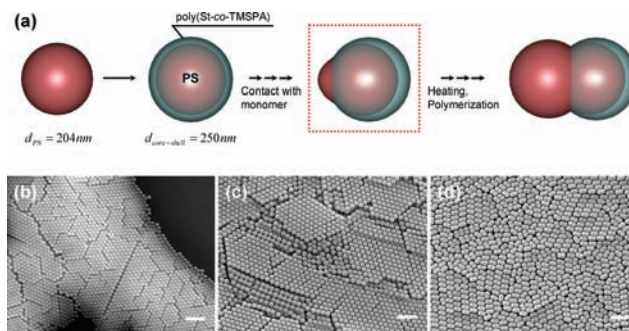


Figure 1. Synthesis of dumbbell-shaped polymer nanoparticles: (a) Schematic representation of two-step seeded emulsion polymerization. (b–d) Scanning electron micrographs of (b) PS nanoparticles, (c) PS/poly(St-co-TMSPA) core-shell nanoparticles, and (d) symmetric dumbbell-shaped nanoparticles. For the synthesis of (d), $V_m/V_{\text{core-shell}}$, the volume ratio of the monomer solution to the core-shell seed particles, was 0.9. The scale bars in the micrographs represent 1.0 μm .

min and then centrifuging. When the aqueous suspension of PS nanoparticles was mixed with toluene (PS + toluene), the PS nanoparticles absorbed all of the toluene and creamed to the top of the mixture, as shown in Figure 2a. In contrast, the poly(St-co-TMSPA) nanoparticles absorbed very little toluene and formed a sediment at the bottom. Interestingly, the core-shell nanoparticles also absorbed very little toluene. However, this slight swelling resulted in a dramatic change to the particle morphology. Scanning electron micrographs of the dried swollen particles show that the core-shell nanoparticles were phase-separated into two distinct domains, as shown in Figure 2b. The resulting particles were also highly uniform in size. The structure was unchanged when the core-shell particles were allowed to swell with toluene for 24 h.

We exploited this phase separation to synthesize nonspherical nanoparticles with larger aspect ratios. First, we swelled the core-shell particles with styrene monomer to the intermediate structure shown in Figure 2. Highly monodisperse dumbbell-shaped nanoparticles were then formed upon heating and polymerization.

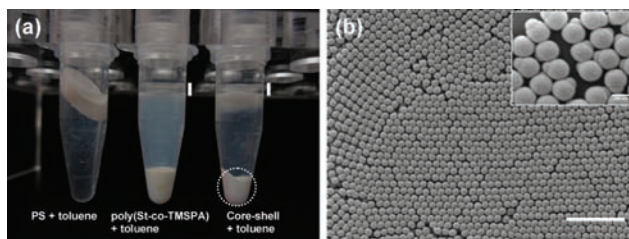


Figure 2. Comparison of particles' capability to swell with toluene: (a) photographs of mixtures of aqueous nanoparticle suspensions with toluene; (b) scanning electron micrographs of the nanoparticles taken from the sediment of the core-shell + toluene mixture. The picture in (a) was taken after centrifugation at 15000g for 20 min. Vertical white bars indicate the toluene layer. The inset in (b) is a scanning electron micrograph of (b) with higher resolution. The scale bar represents 1.0 μm .

[†] Department of Mechanical Engineering.

[‡] Department of Chemical Engineering.

[§] Department of Physics.

^{||} Department of Cell Biology.

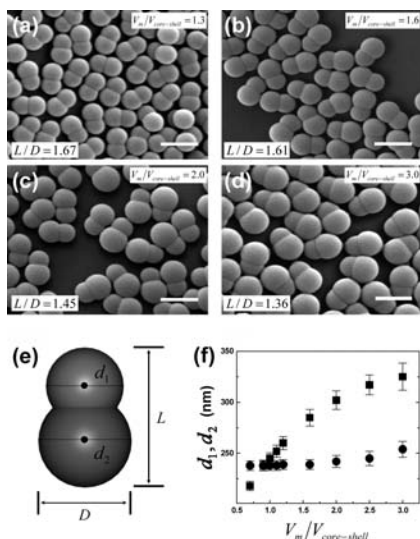


Figure 3. Effect of varying $V_m/V_{\text{core-shell}}$ on the particle geometry: (a–d) Examples of asymmetric dumbbell-shaped nanoparticles prepared with $V_m/V_{\text{core-shell}} =$ (a) 1.3, (b) 1.6, (c) 2.0, and (d) 3.0. (e) Definitions of geometrical parameters describing particle shape. (f) Plots of d_1 (●) and d_2 (■) vs $V_m/V_{\text{core-shell}}$. The error bars indicate the standard deviations of domain sizes measured with scanning electron microscopy. The scale bars in the scanning electron micrographs represent $0.5 \mu\text{m}$.

We were able to control the relative sizes of the two lobes by varying $V_m/V_{\text{core-shell}}$, the ratio of the volumes of swelling monomer and core-shell seed particles in the second step, from 0.75 to 3.0. Figure 3a–d shows scanning electron micrographs of the particles with $V_m/V_{\text{core-shell}} = 1.3, 1.6, 2.0,$ and 3.0 , respectively. All of the batches displayed high uniformity in size and shape. The diameters of the two lobes, d_1 and d_2 , are plotted against the swelling ratio $V_m/V_{\text{core-shell}}$ in Figure 3f. Interestingly, only one of the two lobes seemed to be affected by swelling. On the basis of the swelling behavior of the PS, copolymer, and core-shell particles in Figure 2, we conclude that the monomer causes the non-cross-linked PS core to locally squeeze past the hydrophilic copolymer shell and preferentially absorb all of the additional monomer during polymerization. This is illustrated in the third and final stages of the polymerization outline shown in Figure 1a.

This approach for synthesizing nonspherical nanoparticles is not only robust but also produces high yields. After polymerization, a typical batch of symmetric dumbbell-shaped particles contains about 10^{13} particles mL^{-1} with >99% conversion. These volumes can be easily scaled without any sorting process.

The ability to produce large quantities of uniform dumbbell-shaped nanoparticles enables the formation of distinctively structured thin films. We cast thin films of dumbbells using vertical evaporative deposition. The resulting films had large macroscopic domains of uniform thickness and morphology. Each domain was long and thin, with its narrow dimension roughly parallel to the direction of deposition, as indicated by the arrow in Figure 4. The domains exhibited striking thickness-dependent morphologies. In the thinnest regions of the film (Figure 4a), the particles formed a polycrystalline monolayer with the long axis of each particle parallel to the substrate; we refer to this orientation as “down”. As the film thickness increased, the particles became oriented “up” to form a polycrystalline monolayer (Figure 4b). As the thickness increased further, the film began to form polycrystalline bilayers with down–down (Figure 4c), down–up (Figure 4d) and up–up (Figure 4e) orientations. When the film thickness exceeded more than two upright layers, it failed to crystallize, as shown in Figure 4f.

In conclusion, we have found that nonspherical dumbbell-shaped nanoparticles can readily be synthesized by emulsion polymerization

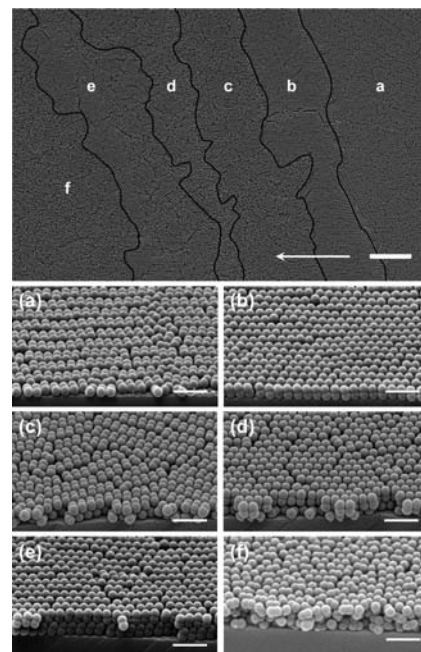


Figure 4. Symmetric dumbbell-shaped nanoparticles self-assemble into distinctive thickness-dependent structures. (top) Top-view electron micrograph of the dried film with labeled domains. The scale bar represents $5.0 \mu\text{m}$; the arrow indicates the direction of deposition. (a–f) Side-view electron micrographs of the labeled domains in the top panel ($1.0 \mu\text{m}$ scale bars).

without cross-linking of seed particles. The synthetic strategy we have demonstrated is valid not only in the variation of geometry but also in the synthesis of amphiphilic nanoparticles. The morphology of these particles has a dramatic impact on the structure of self-assembled films. Ultimately, we expect that these particles may provide a novel building block in three-dimensional photonic crystals.

Acknowledgment. We acknowledge support from the National Institute for Nano Engineering at Sandia National Laboratory, an NSF CAREER Grant to E.R.D. (CBET-0547294), and seed funding from the Yale NSF MRSEC (DMR-0520495).

Supporting Information Available: Additional experimental details. This material is available free of charge via the Internet at <http://pubs.acs.org>.

References

- (a) Yang, Z.; Huck, W. T. S.; Clarke, S. M.; Tajbakhsh, A. R.; Terentjev, E. M. *Nat. Mater.* **2005**, *4*, 486. (b) He, T.; Adams, D. J.; Butler, M. F.; Yeoh, C. T.; Cooper, A. I.; Rannard, S. P. *Angew. Chem., Int. Ed.* **2007**, *46*, 9243.
- (a) Xia, Y.; Gates, B.; Li, Z. Y. *Adv. Mater.* **2001**, *13*, 409. (b) Velikov, K. P.; van Dillen, T.; Polman, A.; van Blaaderen, A. *Appl. Phys. Lett.* **2002**, *81*, 838. (c) Birner, A.; Wehrspohn, R. B.; Gösele, U. M.; Busch, K. *Adv. Mater.* **2001**, *13*, 377.
- (a) Letz, M.; Schilling, R.; Latz, A. *Phys. Rev. E* **2000**, *62*, 5173. (b) Chong, S. H.; Götz, W. *Phys. Rev. E* **2002**, *65*, 041503. (c) Vega, C.; Monson, P. A. *J. Chem. Phys.* **1997**, *107*, 2696. (d) Yethiraj, A.; van Blaaderen, A. *Nature* **2003**, *421*, 513.
- (a) Manoharan, V. N.; Elsesser, M. T.; Pine, D. J. *Science* **2003**, *301*, 483. (b) Kraft, D. J.; Vluc, W. S.; van Kats, C. M.; van Blaaderen, A.; Imhof, A.; Kegel, W. K. *J. Am. Chem. Soc.* **2009**, *131*, 1182.
- Johnson, P. M.; van Kats, C. M.; van Blaaderen, A. *Langmuir* **2005**, *21*, 11510.
- (a) Sheu, H. R.; El-Aasser, M. S.; Vanderhoff, J. W. *J. Polym. Sci., Part A: Polym. Chem.* **1990**, *28*, 629. (b) Chen, Y. C.; Dimonie, V.; El-Aasser, M. S. *Macromolecules* **1991**, *24*, 3779. (c) Kim, J. W.; Larsen, R. J.; Weitz, D. A. *J. Am. Chem. Soc.* **2006**, *128*, 14374.
- Mock, E. B.; De Bruyn, H.; Hawkett, B. S.; Gilbert, R. G.; Zukoski, C. F. *Langmuir* **2006**, *22*, 4037.
- (a) Tissot, I.; Novat, C.; Lefebvre, F.; Bourgeat-Lami, E. *Macromolecules* **2001**, *34*, 5737. (b) Bourgeat-Lami, E.; Tissot, I.; Lefebvre, F. *Macromolecules* **2002**, *35*, 6185.

JA101760Q